CODEN STJSAO
ZX470/1509

ISSN 0562-1887
UDK 662.61:662.944:662.753.3:536.2:519.63(043)

Thermodynamic Analysis of Heat and Mass Transfer in the Combustion Chamber of an Industrial Furnace

Igor BONEFAČIĆ, Paolo BLECICH and ***Igor WOLF***

Tehnički fakultet Sveučilišta u Rijeci
(Faculty of Engineering, University of Rijeka),
Vukovarska 58, HR-51000 Rijeka,
Republic od Croatia

igor.bonefacic@riteh.hr

Preliminary note

CFD analysis of heavy fuel oil combustion in a 6.7 MW cylindrical vertically-fired furnace has been carried out. The furnace supplies process heat in the Oil refinery of the National oil company (INA) in Rijeka-Croatia. The motivation of the work was to improve the performance of the combustion process by changing fuel and burner parameters. The commercial CFD-code Fluent is used to model transport and reaction in the furnace. The chosen CFD models for heavy fuel oil spray combustion are compared with measurement data found in the literature and good agreement is achieved. The combustion process is investigated through the influence of different parameters: air excess ratio, fuel oil droplet diameter, spray cone half-angle and burner swirl number. It is determined that the best performance of the combustion process is achieved for an air excess ratio of 1.15. The droplet diameter should be neither too small nor too large: medium-sized droplets (~100 μm) mix well with air and reside in the furnace the right amount of time for complete burnout to occur. Small spray cone half-angles deteriorate mixing between air and fuel which is reflected in higher CO concentrations. The burner's swirl number influences the mixing rate of air and fuel: a small swirl number is not desired as it elongates the flame, increases flue gases temperatures and reduces the furnace heating output.

Keywords
Burner swirl number
Droplet diameter
Heavy fuel oil
Industrial furnace
Spray cone half-angle

Termodinamička analiza prijenosa topline i tvari u komori izgaranja industrijske peći

Prethodno priopćenje

U radu je računalnim putem analizirano izgaranje teškog lož-ulja u vertikalnoj cilindričnoj peći učinka 6.7 MW. Peć snabdijeva INA-inu rafineriju nafte u Rijeci procesnom toplinskom energijom. Motivacija rada je bilo poboljšavanje procesa izgaranja promjenom svojstva raspršivanja goriva i parametara plamenika. Komercijalni CFD-kod Fluent korišten je za modeliranje transporta i kemijskih reakcija u peći. Rezultati CFD modela za izgaranje teškog lož-ulje uspoređeni su s, u literaturi, pronađenim podacima mjerenja, a postignuto slaganje je zadovoljavajuće. Proces izgaranja istraživan je putem utjecaja različitih parametara: koef. pretička zraka za izgaranje, promjera kapljica teškog lož-ulja, polukuta konusa raspršivanja i vrtložnog broja plamenika. Utvrdilo se da se najbolji proces izgaranja postiže za vrijednost koef. pretička zraka od 1.15. Promjer kapljica lož-ulja ne smije biti niti premalen niti prevelik: kapljice srednje veličine (~100 μm) dobro se miješaju sa zrakom i dovoljno dugo borave u peći da potpuno izgore. Mali polukut konusa raspršivanja pogoršava miješanje između zraka i goriva što se odražava s višim koncentracijama CO-a. Vrtložni broj plamenika utječe na brzinu miješanja zraka i goriva: mali vrtložni broj nije poželjan jer izdužuje plamen, povećava temperaturu dimnih plinova i smanjuje toplinski učinak peći.

Ključne riječi
Industrijska peć
Polukut konusa raspršivanja
Promjer kapljice
Teško lož-ulje
Vrtložni broj plamenika

Received (primljeno): 2009-09-01
Accepted (prihvaćeno): 2011-04-25

1. Introduction

Although concern on global climate changes grows, fossil fuels are still the major energy source in the world. The conversion of fossil fuels into energy is inevitably accompanied by a combustion process which, apart from useful heat, generates flue gases that are harmful both to humans and to the environment. Liquid fossil fuels are being burnt in large power plants to generate electricity, in vehicles, ships and airplanes to generate mechanical work, or in buildings to heat air and water. Design of furnaces and burners for the combustion of liquid fossil fuels and the analysis of combustion processes involving liquid fuels are still a frequently addressed field of research.

While once the analysis of combustion in energy conversion systems was confined to measurements and observations, recently developed and commercially

Symbols/Oznake

A	- area, m^2 površina
AER	- air excess ratio koeficijent pretička zraka
C_v	- vapor concentration, $kmol \cdot m^{-3}$ - koncentracija pare
d	- diameter, μm - promjer
f	- mixture fraction - udio smjese
h	- heat transfer coefficient, $W \cdot m^{-2} \cdot K^{-1}$ - koef. prijelaza topline
k	- turbulent kinetic energy, $m^2 \cdot s^{-2}$ - turbulentna kinetička energija
N_v	- vapor molar flux, $kmol \cdot m^{-2} \cdot s^{-1}$ - molni protok pare
PDF	- probability density function - funkcija gustoće vjerojatnosti
Q_h	- furnace heating output, MW - toplinski učin peći
RKE	- realizable k-ε turbulence model - realistični k-ε model turbulencije
RSM	- Reynolds stress model - Reynoldsov model naprezanja
S	- swirl number - vrtložni broj
SKE	- standard k-ε turbulence model - standardni k-ε model turbulencije
T	- temperature, K - temperatura
u	- velocity, $m \cdot s^{-1}$ - brzina
WSGGM	- weighted sum-of-gray-gases model - model ponderirane sume sivih plinova

Greek letters/Grčka slova

ε	- turbulent dissipation rate, $m^2 \cdot s^{-3}$ - turbulentna disipacija
κ_c	- mass transfer coefficient, $m \cdot s^{-1}$ - koef. prijenosa tvari
φ	- spray cone half-angle, ° - polukut konusa raspršivanja
σ	- Stefan-Boltzmann constant, $5.67 \cdot 10^{-8}$ $Wm^{-2}K^{-4}$ - Stefan-Boltzmannova konstanta

Subscripts/Indeksi

bp	- boiling point - točka vrenja
D	- droplet - kapljica
g	- flue gases - dimni plihovi
vap	- vaporization - isparivanje
∞	- free stream - slobodna struja

available computer combustion codes became indispensable especially when analyzing and optimizing combustion processes with pulverized coal, fuel oil sprays and gaseous fuels.

Computer modeling of the complex physical and chemical mechanism of liquid fuel combustion includes numerical solutions for multidimensional, steady or transient, differential equations for the conservation of mass, momentum and energy. A number of submodels need to be coupled within this procedure: turbulence-chemistry interaction, heat and mass interaction between discrete and continuous phase, radiative heat transfer, NO_x, SO_x and soot formation.

Transport, dispersion, evaporation and combustion of liquid fuel droplets and sprays are investigated in [1-2]. Several papers carry out numerical and experimental studies of heavy fuel oil spray combustion in cylindrical furnaces [3-5]. Barreiros et al. [3] underline the influence of the burner geometry and air inlet velocities on final gas temperatures, gas velocities and on species concentration in the furnace. They report NOx concentrations as a function of the burner swirl number and conclude that fast droplet evaporation and long residence time contribute NOx reduction. Byrnes et al. [4] obtained good predictions of gas temperatures, CO_2, CO, O_2 and NO concentrations as well as particulate emissions for five flames with different air excess ratios, swirl numbers, primary air excess ratios and atomizer cup speeds. Saario et al. [5] stress that the standard k-ε (SKE) turbulence model cannot predict faithfully the highly swirling flow field and that the Reynolds stress model (RSM) should be used instead. They concluded that the RSM model is capable of producing reasonably good predictions for O_2, CO_2, CO and NO concentrations, except in the near burner region. Wu et al. [6] investigated the contribution of the number, location, type and firing mode of fuel oil atomizers on NO emissions reduction in an industrial burner with heavy fuel oil combustion and highly

preheated air. They concluded that, among other possible setups, double-mixed-vortex atomizers with a single direct-into-furnace fuel injection firing mode reduce NO emissions.

The cylindrical vertically-fired furnace of the National oil company (INA) refinery in Rijeka has a nominal power of 6.7 MW and supplies heat for the process of oil vacuum distillation. The radiation chamber of the furnace is 7 m high and 2.8 m in diameter, followed by a conical section that directs flue gases into the chimney. Three highly swirling burners are placed at the bottom of the combustion chamber and spray heavy fuel oil or gaseous fuel bottom-up.

The finite-volume based commercial code Fluent 6 is employed to simulate heavy fuel oil spray combustion in the INA's furnace. Unfortunately, measurements of the combustion process in the INA's furnace have not been undertaken as probing of the furnace was not allowed and only effluent measurements would have been possible. Nevertheless, the combustion models are verified against existing measurements for heavy fuel oil spray combustion found in the literature [5]. The measurement data in [5] include CO_2, O_2 and CO concentrations for a cylindrical down-fired laboratory furnace at several positions. Thereafter, the CFD analysis is extended to the INA's furnace with the goal of enhancing the furnace performance and reducing SO_x and CO emissions by varying fuel and burner parameters.

2. Modeling fuel oil spray combustion

The turbulent flow of the gas phase in the combustion chamber of the furnace is governed by the equations for the conservation of mass, momentum and energy. These partial differential equations are approximated by algebraic equations for a finite number of volumes in the domain [7]. The linkage between continuity and momentum equations is performed through SIMPLE-based methods. The momentum equations require additional relationships to account for turbulence effects in the gas phase flow. Turbulence closure models for momentum equations in reacting and highly swirling flows are reviewed in [8]. Although the standard k-ε turbulence model is the most widely used approach for fluid dynamics problems, its major shortcoming is the assumption that turbulence is isotropic. This limitation may seriously affect the results in highly swirling flows. Nevertheless, several variants of the k-ε model are developed to account for swirling and strained flow effects. The renormalization group (RNG) model includes swirling effects and could offer improved accuracy for rotating flows, though there is no general agreement in this regard. The realizable k-ε (RKE) model predicts more accurately the spreading rate of planar and round jets, thus providing better results for flows involving rotation, separation and recirculation [9]. The RSM model solves directly the Reynolds stress terms in the momentum equations and produce better results than the k-ε models for highly non-isotropic turbulent flows, though it is more computationally intensive. For flows with swirl numbers $S<0.5$ both the RNG k-ε model and the realizable k-ε model yield appreciable improvements over the standard k-ε model. For highly swirling flows ($S>0.5$) the RSM model is recommended [9].

Three turbulence models, namely the SKE, the RKE and the RSM are tested against measurement data of species concentration for heavy fuel oil spray combustion in the cylindrical down-fired laboratory furnace [5].

In non-premixed combustion, fuel and air enter the flame region separately and reaction begins when mixing occur at molecular level. The probability density function (PDF) approach is convenient when the mixing time scale is much longer than the reaction time scale. The PDF approach defines the mixture fraction f as the mass fraction of the primary stream

$$f = \frac{m_{\mathrm{p}}}{m_{\mathrm{p}} + m_{\mathrm{s}}}. \tag{1}$$

Where the primary stream p is the fuel and the secondary stream s is the oxidizer. The conserved scalars, such as fluid density and temperature, can be expressed as a function of the mixture fraction f. Transport equations are written for time-averaged mixture fraction and its variance, analogously to the equations in the standard k-ε turbulence model. In Fluent 6, the PDF model is offered as a pre-processing tool. After fuel composition and boundary values are defined, chemistry calculations are performed and the relationships between gas scalar variables or species mass fractions and mixture fraction or its variance are stored in look-up tables.

Radiative heat transfer in the furnace is solved using the discrete ordinates (DO) heat radiation model. In the DO model the entire solid angle of a control volume is divided into a finite number of angular spans for which the radiative heat transfer equation is discretized. Fuel droplets evaporate relatively quickly and influence radiative heat transfer only in the near-burner region. The weighted sum-of-gray-gases (WSGGM) model is used to determine the absorption coefficient of the gas phase.

An atomizer ejects heavy fuel oil at the burner opening and the swirling flow promotes dispersion and mixing of fuel droplets with the oxidizer in the furnace. Oil droplets heat up to evaporate, boil and eventually react with the oxidizer. In the Lagrangian formulation, the gas phase is modeled using the previously mentioned approaches. Fuel oil droplets, which move through the gas phase along trajectories, are modeled using the following partial differential equations for the conservation of mass, momentum and energy

$$\frac{\mathrm{d}m_\mathrm{D}}{\mathrm{d}t} = -G_\mathrm{D}, \tag{2}$$

$$m_\mathrm{D}\frac{\mathrm{d}u_\mathrm{D}}{\mathrm{d}t} = \sum F_\mathrm{D}, \tag{3}$$

$$\frac{\mathrm{d}(m_\mathrm{D}\cdot i_\mathrm{D})}{\mathrm{d}t} = \sum Q_\mathrm{D}. \tag{4}$$

The mass of the fuel oil droplet m_D changes by the rate G_D because of vaporization. The velocity of the fuel droplet u_D changes because of external forces F_D such as gravity and drag. The droplet enthalpy ($m_\mathrm{D}\cdot i_\mathrm{D}$) changes when heat transfer and reaction with the gas phase occur. The dispersion of particles in the turbulent gas phase is predicted using the stochastic tracking (discrete random walk) model that accounts for the fluctuating component of the gas velocity. The average droplet trajectory in the gas phase is computed from a number of representative particles.

Until the droplet temperature reaches the vaporization temperature ($T_\mathrm{D} < T_\mathrm{vap}$), the equation for droplet inert heating is applied

$$m_\mathrm{D}c_\mathrm{D}\frac{\mathrm{d}T_\mathrm{D}}{\mathrm{d}t} = hA_\mathrm{D}(T_\infty - T_\mathrm{D}) + \varepsilon_\mathrm{D}A_\mathrm{D}\sigma(T_\mathrm{R}^4 - T_\mathrm{D}^4). \tag{5}$$

In equation (5) the change of droplet temperature is related to convective and radiative heat transfer. The vaporization temperature has no physical meaning yet it is a modeling parameter. The heat transfer coefficient is evaluated using the Ranz-Marshall correlation [10]

$$h = \frac{k_\infty}{d_\mathrm{D}}\left[2 + 0.6\,\mathrm{Re}_\mathrm{d}^{1/2}\,\mathrm{Pr}^{1/3}\right]. \tag{6}$$

When the droplet temperature has reached vaporization temperature but remains below boiling temperature ($T_\mathrm{vap} < T_\mathrm{D} < T_\mathrm{bp}$), droplet vaporization is governed by the gradient of fuel vapor concentration between droplet surface and gas phase

$$N_\mathrm{v} = \kappa_\mathrm{c}(C_\mathrm{v,D} - C_\mathrm{v,\infty}). \tag{7}$$

The mass transfer coefficient κ_c is calculated from the Sherwood number [10]

$$\kappa_\mathrm{c} = \frac{D_\mathrm{v,\infty}}{d_\mathrm{D}}\left[2 + 0.6\,\mathrm{Re}_\mathrm{d}^{1/2}\,\mathrm{Sc}^{1/3}\right]. \tag{8}$$

During vaporization, the expression for droplet temperature (5) is expanded with the term for latent heat transfer ($r\cdot\mathrm{d}m_\mathrm{D}/\mathrm{d}t$). When the droplet temperature reaches the boiling point temperature ($T_\mathrm{D} \geq T_\mathrm{bp}$) and assuming constant droplet temperature during boiling, the droplet temperature becomes

$$-r\frac{\mathrm{d}m_\mathrm{D}}{\mathrm{d}t} = hA_\mathrm{D}(T_\infty - T_\mathrm{D}) + \varepsilon_\mathrm{D}A_\mathrm{D}\sigma(T_\mathrm{R}^4 - T_\mathrm{D}^4). \tag{9}$$

For heavy fuel oil, the vaporization and the boiling point temperatures are 400 K and 589 K, respectively.

Complete evaporation of fuel oil droplets is assumed, i.e. no coke particles (cenospheres) form after droplet burnout. Coalescence and break-up of oil droplets are neglected, as the discrete phase is dilute and dispersed in the gas phase.

3. Verification of the combustion model

The numerical model for spray combustion of heavy fuel oil is verified against measurement data collected in the cylindrical down-fired laboratory furnace [5]. The measurement data comprises of O_2, CO_2 and CO concentrations. Details on the burner arrangement may be found in [5]. Boundary conditions for the fuel and the oxidizer stream as well as the burner operating conditions are reported in Table 1.

Table 1. Heavy fuel oil composition and properties, burner characteristics in the laboratory furnace [5]

Tablica 1. Sastav i svojstva teškog lož-ulja te radne karakteristike plamenika u laboratorijskoj peći [5]

Heavy fuel oil composition / Sastav teškog lož-ulja	
Carbon / Ugljik, %	85.0
Hydrogen / Vodik, %	11.2
Nitrogen / Dušik, %	0.4
Sulfur / Sumpor, %	3.4
Ash / Pepeo, %	0.034
Heavy fuel oil properties / Svojstva teškog lož-ulja	
Lower heating value / Donja ogrjevna moć, MJ·kg^{-1}	42.1
Mass flow rate / Maseni protok, kg·h^{-1}	12
Temperature / Temperatura, K	373
Injection velocity / Brzina ubrizgavanja, m·s^{-1}	35
Injection angle / Kut ubrizgavanja, °	4 – 12
Droplet diameter / Promjer kapljice, μm	26.8
Atomizer properties / Karakteristike raspršivača	
Air temperature / Temperatura zraka, K	293
Air mass flow rate / Maseni protok zraka, kg·h^{-1}	14.4
Air axial velocity / Aksialna brzina zraka, m·s^{-1}	52.4
Burner properties / Karakteristike plamenika	
Air temperature / Temperatura zraka, K	293
Air mass flow rate / Maseni protok zraka, kg·h^{-1}	173.3
Air axial velocity / Aksialna brzina zraka, m·s^{-1}	17.9
Swirl number / Vrtložni broj, -	1.1

Heavy fuel oil combustion in the test furnace is reduced to a two-dimensional axysimmetric swirl problem. The 2D domain consists of about 10 000 quadrilateral cells. The flame region is refined with about 50 000 cells to test the mesh size influence on final results. Since it was seen that the results are only slightly affected by the grid size, the coarse grid without additional refinement is employed for model verification. Three turbulence models are used to model the highly swirling turbulent flow in the test furnace: the standard k-ε model (SKE), the realizable k-ε model (RKE) and the Reynolds stress turbulence model (RSM). The results of these turbulence models, in terms of CO_2 and O_2 concentrations at different distances from the furnace roof, are compared with measured concentrations, as shown in Figure 1 and 2. Measurement data for temperatures and flow velocities in the test furnace are not provided in [5]. Nevertheless, judging only from species concentrations data, altogether the RSM model produces better results than both the SKE and the RKE turbulence model. Still, the predictions obtained with the RSM model diverge from measurements in the near-burner region and in the vicinity of the furnace axis. The discrepancy between measurement data and numerical predictions in the near-burner region is most likely caused by difficulties in the modeling of the penetration of the heavy oil fuel jet inside the swirl-generated recirculation zone in front of the burner. The penetration depth of the fuel jet inside the recirculation zone is underpredicted by the SKE and the RKE turbulence model. At x = 20 mm, this causes CO_2 concentrations to be underpredicted near the furnace axis and to be overpredicted when approaching the furnace wall. The RSM turbulence model predicts quite well CO_2 concentrations for x = 20 mm, except in the vicinity of the furnace axis. At x = 320 mm and 620 mm, both the SKE and the RKE turbulence models predict constant CO_2 concentrations throughout the radial distance from the furnace axis, but slightly overpredicted. The RSM model overpredicts CO_2 concentrations as well, however better accordance is achieved, especially at x = 320 mm.

At x = 20 mm, O_2 concentrations are underpredicted in all but the RSM turbulence model. As in the case of CO_2 concentrations at x = 320 mm and x = 620 mm, the RKE model and the SKE model predict constant O_2 concentrations throughout the whole radial distance that are in satisfactorily accordance with measurements. Unlike the RKE and the SKE model, the RSM model seems to be partially successful in reproducing the rising O_2 concentration at x = 320 mm as approaching to the furnace wall. CO concentrations are not reported here, but again the predictions of RSM model are superior to the ones of the RKE and the SKE model. Apart from the turbulence model, the predicted values for species fractions in the furnace depend also on the combustion model, on the interaction between discrete and continuous phase and on the boundary conditions.

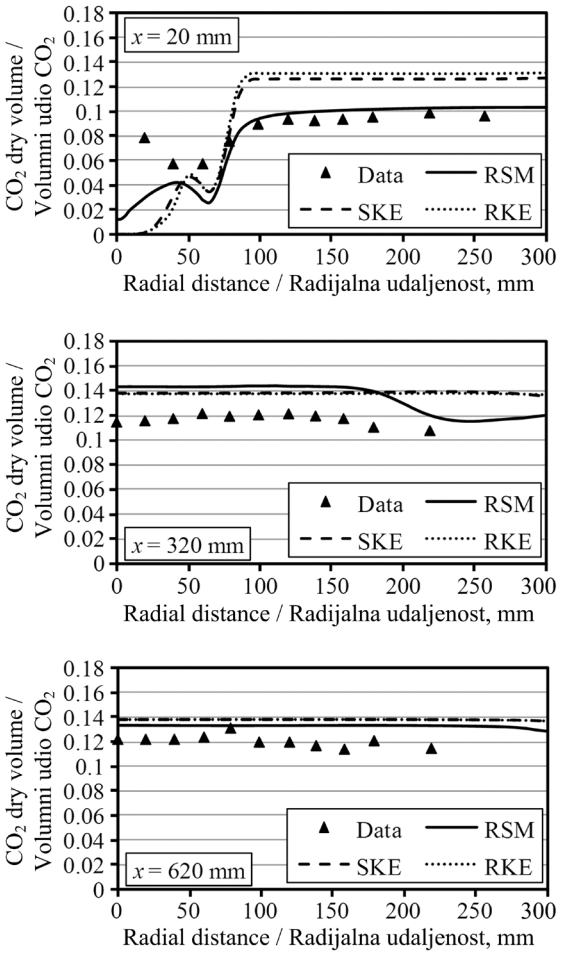

Figure 1. Comparison between predicted CO_2 dry volume fractions and measurements from [5]

Slika 1. Usporedba između numeričkim putem dobivenih volumnih udjela CO_2 i mjerenja iz [5]

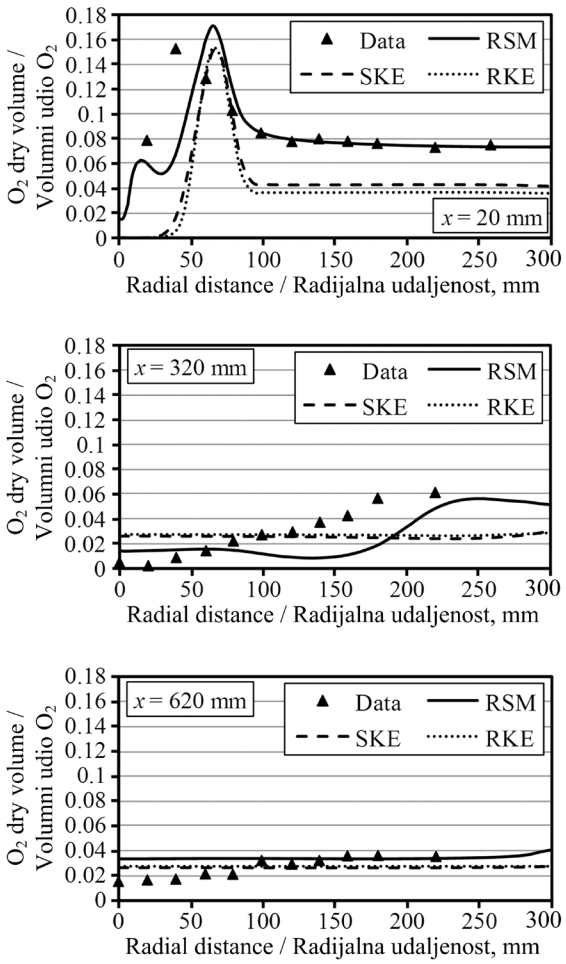

Figure 2. Predicted O_2 volume fraction [%] and measurement data from [5]

Slika 2. Numeričkim putem dobiveni volumni udjeli O_2 i mjerni podaci iz [5]

4. Heavy fuel oil combustion in the INA's industrial furnace

4.1. The INA's industrial furnace

The INA's industrial furnace is a 6.7 MW cylindrical vertically-fired furnace that burns heavy fuel oil or gaseous fuel and supplies heat for the process of oil vacuum distillation [11]. Three highly swirling burners are placed at the bottom of the furnace, each 0.8 m distant from the furnace axis and with 120° radial shift from the other two neighboring burners. The radiation chamber of the furnace is 7 m high and 2.8 m in diameter, followed by a conical constriction section that runs flue gases into the chimney, Figure 3. Heavy fuel oil is brought in the furnace at a mass flow rate of 837 kg/h, at a temperature of 110 °C.

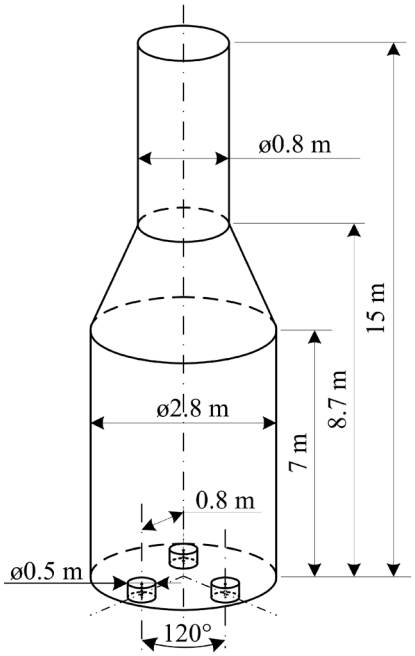

Figure 3. Scheme of the INA's vertical industrial furnace (dimensions not to scale)

Slika 3. Shema INA-ine vertikalne industrijske peći (dimenzije nisu u mjerilu)

Heavy fuel oil is pressurized to 6 bar and, prior to spraying, mixed with water steam at 7.5 bar and 300 °C. The necessary air for combustion is preheated to 180 °C before entering the burners. Heavy fuel oil properties are given in Table 2.

The influence of different parameters on the combustion process in the INA's furnace is studied. Different air excess ratios are selected to investigate the relationship between excess air and both species concentration such as CO, H_2, SO_x and the furnace heating output. The influence of fuel oil droplet diameter and the influence of spray cone half-angle on species concentrations and furnace heating output are also investigated.

The fuel oil droplet diameter changes with the vapor pressure, but to adjust the spray cone half-angle, the atomizer head needs to be replaced. The quality of the combustion process, in terms of furnace heating output, flue gases temperatures and species concentrations leaving the furnace are studied.

Spray combustion of heavy fuel oil is modeled using the previously mentioned transport and reaction models. The swirl number in the INA's industrial furnace is varied from 0.3 to 0.9. The RKE turbulence model is applied for small swirl numbers ($S < 0.5$) because it is less computationally intensive than the RSM model. Also, it has been determined that the two turbulence models produce results within 5% difference when the swirl number is small. The RSM turbulence model is used for high swirl numbers ($S > 0.5$).

Table 2. Heavy fuel oil properties in the INA's industrial furnace

Tablica 2. Fizikalna svojstva teškog lož-ulja u INA-inoj procesnoj peći

Heavy fuel oil properties / Fizikalna svojstva teškog lož-ulja	
Density / Gustoća (288 K), $kg \cdot m^{-3}$	982.6
Thermal conductivity / Toplinska provodnost (383 K), $W \cdot m^{-1} \cdot K^{-1}$	0.1155
Kinematic viscosity / Kinematska viskoznost (383 K), $m^2 \cdot s^{-1}$	$21 \cdot 10^{-6}$
Latent heat / Latentna toplina, $kJ \cdot kg^{-1}$	211.7
Lower heating value / Donja ogrjevna moć, $MJ \cdot kg^{-1}$	40.68
Higher heating value / Gornja ogrjevna moć, $MJ \cdot kg^{-1}$	43.01
Heavy fuel oil composition / Sastav teškog lož-ulja	
Carbon / Ugljik, %	88.26
Hydrogen / Vodik, %	10.62
Sulfur / Sumpor, %	0.84
Nitrogen / Dušik, %	0.28

In order to speed-up the numerical calculations, a reasonable approach is to identify one-third of the furnace as the computational domain and to apply rotational periodicity to its internal sides, as shown in Figure 4. Therefore, the domain has only one burner with the corresponding fuel and air mass flow rate (Table 2). In other words, if the overall furnace heating output and the quantity of flue gases have to be determined, it is just necessary to triplicate the domain's heating output and the flue gases mass flow. The 3D domain is discretized with 70 000 control volumes in a structured grid. Comparing the results produced by the 70 000-cells grid with the results of finer grids, it has been determined that the chosen number of cells presents a good compromise between results accuracy and CPU processing time.

Uniform temperature of 800 K is prescribed to the furnace base wall. Constant temperature of 850 K is given to the radiation chamber wall, 550 K to the walls in the chimney and 650 K to the conical constriction section. All surfaces are opaque to heat radiation and have an emissivity of 0.8. The discrete phase (fuel oil droplets) is reflected from the furnace surfaces if collision occurs. Fuel oil droplets are injected into the furnace by setting a cone-type injection at the center of the burner. Where not defined explicitly, the oil droplet diameter is 50 μm, the spray cone half-angle 42.5°, the burner swirl number 0.78 and the air excess ratio 1.15.

4.2. Results and discussion

4.2.1. The influence of excess air

The air excess ratio (AER) should be maintained within a narrow range of values. A too small AER results with in increased CO concentrations and larger heat losses due to incomplete combustion. A too big AER increases sensible heat losses in the exhaust flue gases. Seven AERs values (0.9, 0.975, 1.05, 1.125, 1.15, 1.20 and 1.275) are selected to determine the influence of excess air on species concentrations in the furnace and on the furnace heating output.

CO and SO_x (SO_2 and SO_3) concentrations in flue gases at the outlet of the furnace are plotted in Figure 5 as a function of the AER number. It can be seen that the CO concentration decreases and the SO_x concentration increases as more excess air is supplied, that is, as the fuel oil combustion process becomes more complete.

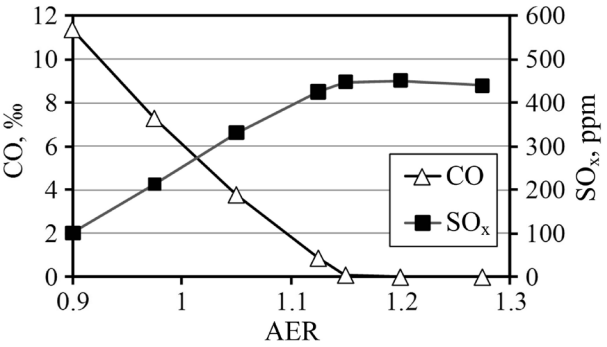

Figure 5. CO and SO_x concentrations as function of AER

Slika 5. CO i SO_x koncentracije u funkciji koef. pretička zraka

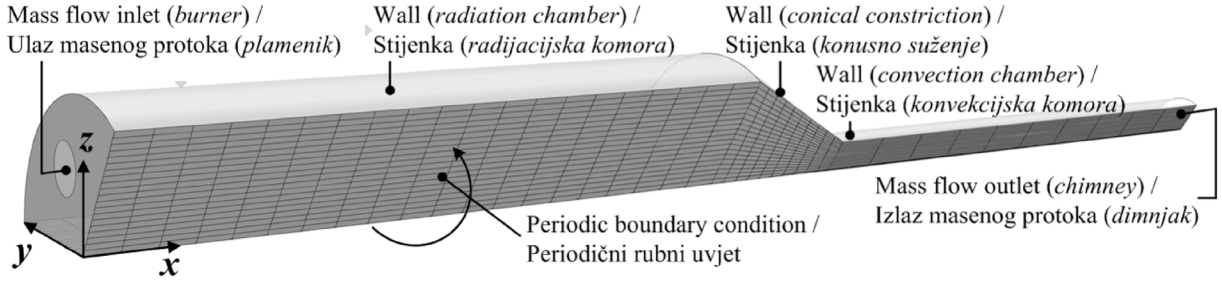

Figure 4. Domain and boundary conditions for modeling heavy fuel oil combustion in the INA's vertical industrial furnace

Slika 4. Domena i rubni uvjeti za modeliranje izgaranja teškog lož-ulja u INA-inoj vertikalnoj industrijskoj peći

At AER = 1.15, the CO concentration drops to 0 and the SO_x concentration reaches its maximum. The furnace heating output Q_h is determined as the total (radiation and convection) heat transfer rate to the radiation chamber walls where the water pipe bundles are placed. Furnace heating output and flue gases temperature T_g at the exit of the radiation chamber are plotted in Figure 6.

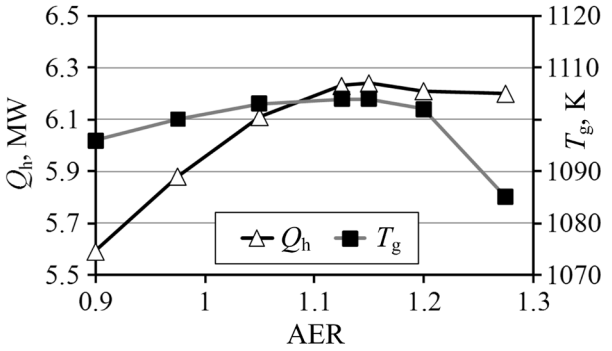

Figure 6. Furnace heating output Q_h and flue gases temperature T_g as function of AER

Slika 6. Toplinski učin peći Q_h i temperatura dimnih plinova T_g u funkciji koef. pretička zraka

Both the heating output and the flue gases temperatures reach a maximum value for an AER of 1.15. As one could expect, a furnace with spray combustion of heavy fuel oil yields overall best performance for an AER around 1.15. Both smaller and larger AERs downgrade the furnace performance because of incomplete combustion and larger sensible heat losses, respectively.

4.2.2. The influence of the fuel oil droplet size

The size of the fuel oil droplet influences the speed of the combustion process. The smaller the oil droplet the larger the contact surface between droplet and air and the better the vaporization and the mixing with the air. A large fuel droplet would need more time to evaporate, thus would start burning later in a region of the furnace with lower temperatures, and would end up leaving the furnace partially unburnt. A relationship between the diameter of heavy fuel oil droplets and the fuel ejection velocity (*x*-axis velocity here) from the atomizer has been proposed in [12] and reads

$$w_D = 1098.8 \cdot d_D^{-0.8}, \tag{9}$$

where w_D is the droplet velocity in m·s^{-1}, and d_D the droplet diameter in μm. Five oil droplet diameters are considered here: 50, 75, 100, 125 and 150 μm. CO and H_2 concentrations in flue gases are plotted in Figure 7 as function of the oil droplet diameter. CO and H_2 concentrations increase significantly for droplet diameters above 100 μm, indicating that incomplete combustion occurs in the furnace.

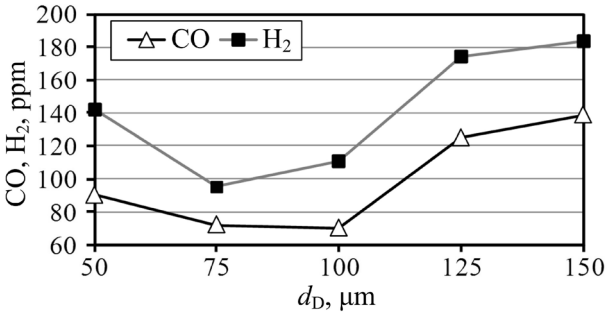

Figure 7. CO and H_2 concentrations as function of fuel oil droplet diameter d_D

Slika 7. CO i H_2 koncentracije u funkciji promjera kapljica lož-ulja d_D

On the other hand, a small fuel oil droplet (d_D = 50 μm) also increases CO and H_2 concentrations. Indeed, a smaller droplet assumes a higher ejection velocity from the atomizer, expression (9), and thus a shorter droplet residence time in the furnace. The shorter the droplet residence time the higher the unburnt fraction in the droplet and the higher the CO and the H_2 concentrations in flue gases. Medium-sized fuel oil droplets lead to maximum heating output of the furnace, and to minimum flue gases temperatures at the exit of the radiation chamber, as shown in Figure 8.

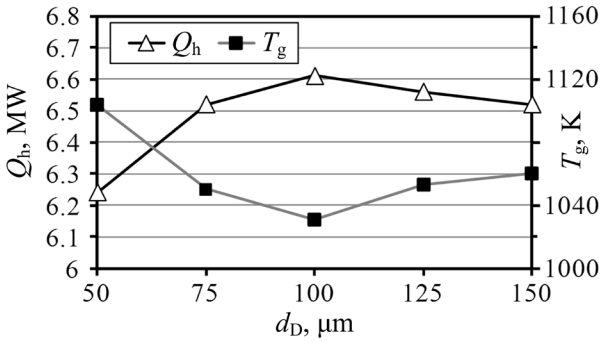

Figure 8. Furnace heating output Q_h and flue gases temperature T_g as a function of droplet diameter d_D

Slika 8. Toplinski učin peći Q_h i temperatura dimnih plinova T_g u funkciji promjera kapljica lož-ulja d_D

4.2.3. The influence of the spray cone half-angle

The atomizer sprays heavy fuel oil droplets in a hollow-cone pattern. Typically, the spray cone half-angle φ ranges from 30° to 70°. A smaller spray cone half-angle produces a narrower but a longer flame. A larger cone half-angle produces a wider but a shorter flame. Four different cone half-angles are considered: 30°, 42.5°, 55° and 67.5°. The influence of the cone half-angle on CO and H_2 concentrations in flue gases at the exit of the furnace is shown in Figure 9. A small cone half-angle leads to an elongated flame with worse mixing between fuel and air and more CO and H_2 in flue gases.

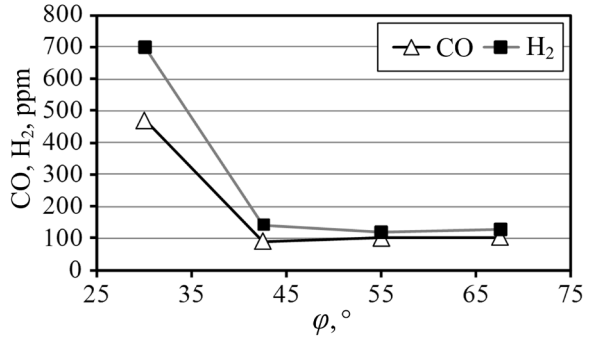

Figure 9. CO and H_2 concentrations as a function of the spray cone half-angle φ

Slika 9. CO i H_2 koncentracije u funkciji polukuta konusa raspršivanja φ

Spray cone half-angles of 42.5° and above present just about even CO and H_2 concentrations, indicating a good mixing between fuel and air. This is reflected on the furnace heating output and on flue gases temperatures at the exit of the radiation chamber, as shown in Figure 10.

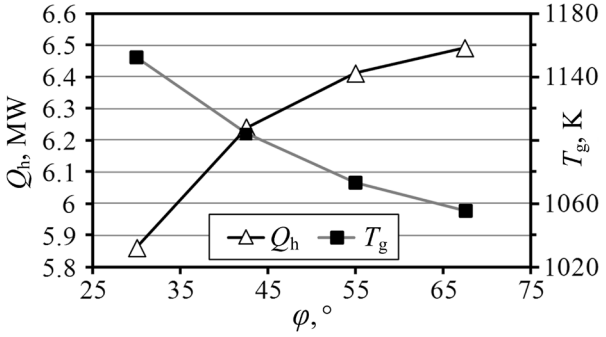

Figure 10. Furnace heating output Q_h and gases temperatures T_g as function of spray cone half-angle φ

Slika 10. Toplinski učin peći Q_h i temperatura plinova T_g u funkciji polukuta konusa raspršivanja φ

4.2.4. The influence of the swirl number

The burner insures a quality combustion process in the furnace by providing the necessary turbulence for mixing of air and fuel. Five different swirl numbers are considered: 0.3, 0.42, 0.6, 0.78 and 0.93. A high swirl number S strengthens the recirculation zone and enhances mixing. Thus, the combustion process produces less CO and H_2 but slightly more SO_x emissions, as shown in Figure 11.

Swirl numbers under 0.6 affect the heating output strongly. The elongated flame that originates at low swirl numbers pushes large quantities of heat directly into the chimney. This causes the furnace heating output to deteriorate and flue gases temperatures to increase, Figure 12. A well-chosen burner swirl number is likely to give the flame a good shape for a high heat transfer rate towards the walls of the radiation chamber.

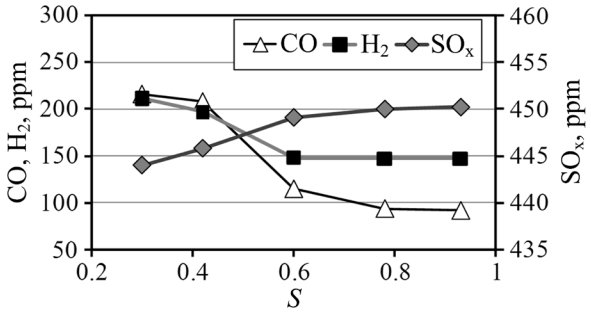

Figure 11. CO, H_2 and SO_x concentrations as function of the burner swirl number S

Slika 11. CO, H_2 i SO_x koncentracije u funkciji vrtložnog broja plamenika S

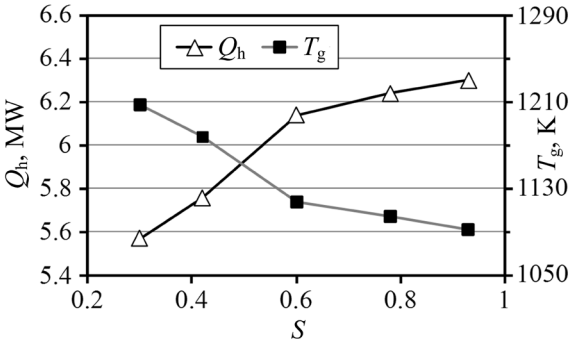

Figure 12. Furnace heating output Q_h and flue gases temperatures T_g as function of the swirl number S

Slika 12. Toplinski učin peći Q_h i temperature dimnih plinova T_g u funkciji vrtložnog broja S

The effect of two burners' swirl numbers – 0.3 and 0.9 on the flow field in the near-burner region is shown in Figure 13. The flow pathlines colored by turbulence intensity present a substantial difference: the high swirl number shortens and intensifies the recirculation zone.

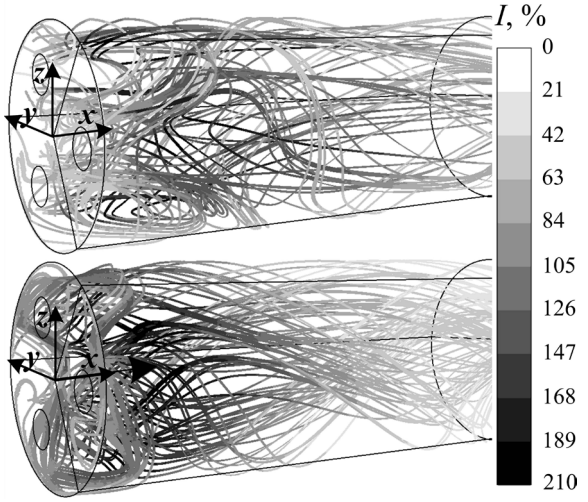

Figure 13. Flow pathlines in the furnace colored by turbulence intensity I at S = 0.3 (above) and S = 0.93 (below)

Slika 13. Strujnice u peći obojane intenzitetom turbulencije I za S = 0.3 i (gore) i S = 0.93 (dolje)

4.2.5. Temperature distributions

Figure 14, 15 and 16 show temperature distributions in the vertical industrial furnace for different cases. A small swirl number originates an elongated flame which decreases the furnace heating output, Figure 14. Higher swirl numbers and larger spray cone half-angles shorten the flame and increase the heating output, Figure 15. Unlike the former two, the flame in Figure 16 has the recirculation zone in front of the burner penetrated by the burner's air stream. This is caused by large fuel droplets which evaporate more slowly and start burning only when pulled back by the recirculating flow in the region about the furnace axis or in the near-wall region.

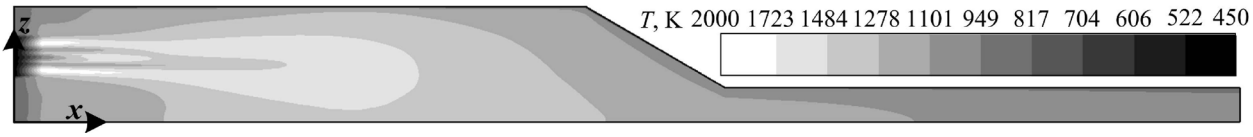

Figure 14. Temperature distributions T_g in the plane of the burner axis for AER = 1.15, $S = 0.30$, $\varphi = 42.5°$ and $d_D = 50$ μm
Slika 14. Raspodjela temperatura T_g u ravnini osi plamenika za koef. pretička zraka 1.15, $S = 0.30$, $\varphi = 42.5°$ i $d_D = 50$ μm

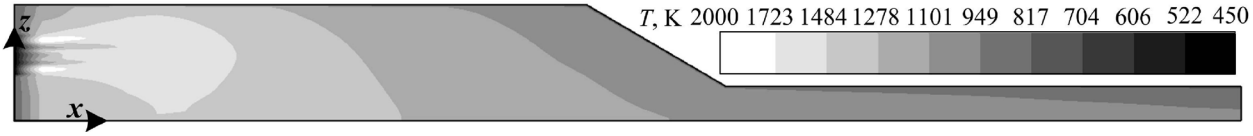

Figure 15. Temperature distributions T_g in the plane of the burner axis for AER = 1.15, $S = 0.78$, $\varphi = 55°$ and $d_D = 50$ μm
Slika 15. Raspodjela temperatura T_g u ravnini osi plamenika za koef. pretička zraka 1.15, $S = 0.78$, $\varphi = 55°$ i $d_D = 50$ μm

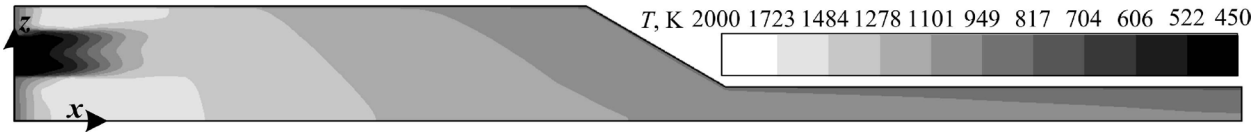

Figure 16. Temperature distributions T_g in the plane of the burner axis for AER = 1.15, $S = 0.78$, $\varphi = 42.5°$ and $d_D = 125$ μm
Slika 16. Raspodjela temperatura T_g u ravnini osi plamenika za koef. pretička zraka 1.15, $S = 0.78$, $\varphi = 42.5°$ i $d_D = 125$ μm

5. Conclusion

Spray combustion of heavy fuel oil in a vertically-fired industrial furnace has been studied numerically. The predictions of the PDF combustion model together with three different turbulence models have been tested against existing measurements. The RSM model produces better predictions of the swirling reactive flow than k-ε-based models, though it is more CPU-intensive.

Fuel and burner parameters such as air excess ratio, fuel oil droplet diameter, burner swirl number and spray cone half-angle have been varied within a range of values to determine their influence on the combustion process. An air excess ratio of 1.15 yields best combustion with minimum unburnt species (CO and H_2) and with maximum furnace heating output. The fuel oil droplet diameter should be neither too small nor too large: droplets with about a 100 μm in diameter yield the highest heating output with small CO concentrations. Smaller droplets travel at high velocity in the furnace and produce more unburnt fractions. Larger droplets affect the mixing rate between air and fuel since the total air-droplet contact surface decreases. The spray cone half-angle should be larger than 40°, since smaller ones increase CO and H_2 concentrations up to 6 times. The burner swirl number has major influence on the shape of the flame and on the mixing rate. Swirl numbers ranging from 0.5 to 1.0 assures good mixing of air and fuel and produce a flame with the proper length.

REFERENCES

[1] BACHALO, W.: *Injection, dispersion and combustion of liquid fuels,* 25th Int Symp on Combustion, The Combustion Institute, 333-371, 1994.

[2] CHIU, H.H.: Advances and challenges in droplet and spray combustion: Toward a unified theory of droplet aerothermochemistry, Progress in Energy and Combustion Science (2000) 26, 381-416.

[3] BARREIROS, A., CARVALHO, M.G., COSTA, M., LOCKWOOD, F.C.: *Prediction of the near burner region and measurements of NOx and particulate emissions in heavy fuel oil spray flames*, Combustion and Flame (1993) 92, 231-240.

[4] BYRNES, M.A., FOUMENYA, E.A., MAHMUDA, T., SHARIFAHA, A.S.A.K., ABBASB, T., COSTENB, P.G., LOCKWOOD, F.C.: *Measurements and predictions of nitric oxide and particulates emissions from heavy fuel oil spray flames,* 26th Int Symp on Combustion, The Combustion Institute, 2241-2250, 1996.

[5] SAARIO, A., REBOLA, A., COELHO, P.J., COSTA, M., OKSANEN, A.: *Heavy fuel oil combustion in a cylindrical laboratory furnace: measurements and modeling*, Fuel (2005) 84, 359-369.

[6] WW, S.-R., CHANG, W.-C., CHIAO, J.: *Low NOx heavy fuel oil combustion with high temperature air*, Fuel (2007) 86, 820-828.

[7] VERSTEEG, H.K., MALALASEKERA, W., *An introduction to computational fluid dynamics, the finite volume method*, Longman Group Ltd., Essex, 1995.

[8] SLOAN, D.G., SMITH, P.J., SMOOT, L.D.: *Modeling of swirl in turbulent flow systems*, Progress in Energy and Combustion Science (1986) 12, 163-250.

[9] EATON A.M., SMOOT, L.D., HILL, S.C., EATOUGH, C.N.: *Components, formulations, solutions, evaluation and application of comprehensive combustion models*, Progress in Energy and Combustion Science (1999) 25, 387-436.

[10] RANZ, W.E., MARSHALL, Jr., W.R..: *Evaporation from drops*, Chemical Engineering Progress (1952) 48(3), 141-146.

[11] BONEFAČIĆ, I.: *Thermodynamic analysis of heat and mass transfer in the combustion chamber of an industrial furnace,* MSc Thesis, Faculty of Engineering, University of Rijeka, Croatia, 2005.

[12] SCHNEIDER, D.R.: *Research on the possible reduction of SO_3 emissions for heavy fuel oil combustion*, PhD Thesis, Faculty of Mechanical Engineering and Naval Architecture, University of Zagreb, Croatia, 2002.